MATEC Web of Conferences **233**, 00006 (2018) https://doi.org/10.1051/matecconf/201823300006
EASN-CEAS 2018

Dynamic Force Analysis of a Novel Mechanism for Chord and Camber Morphing Wing Under Aerodynamic Loading

Harun Levent Şahin[1,*], *Bora Orçun* Çakır[2], and *Yavuz* Yaman[3]

[1]Graduate Research Assistant, Department of Aerospace Engineering, METU, Republic of Turkey
[2]Undergraduate Student, Department of Aerospace Engineering, METU, Republic of Turkey
[3]Professor, Department of Aerospace Engineering, METU, Republic of Turkey

Abstract. In this paper, the dynamic force analysis of a novel deployable mechanism, called as scissor-structural mechanism (SSM), for active camber and chord morphing have been presented. The mechanism is created via combination of several scissor-like-elements (SLEs). With a novel kinematic synthesis concept, various types of scissor-like-elements are assembled together to provide the desired airfoil geometries. The types (translational, polar), the number of scissor-like-elements, their orientations with respect to centerline of the airfoil and their distribution frequencies over the chord length are the design parameters, which allow designers to achieve all the possible geometric shapes. With the assumption of an existing fully-compliant wing skin, it is possible to adjust the wing profile to various desired airfoil geometries. With the help of developed computer routine, the mechanism is generated which yields the minimum possible design error. After the selection of mechanism, the position, velocity and acceleration analyses of the mechanism have been done. In order to prove aerodynamic efficiency of newly created airfoil geometries and obtain pressure distribution over the airfoil, 2D aerodynamic analyses have been done with the package program XFOIL. The flow characteristics used for the analysis are determined by the flight envelope of a generic UAV. Obtained pressure distribution is applied as the lumped force on the joints. By assigning the approximate link masses and mass centers, the dynamic force analysis of the mechanism has also been performed in order to estimate the required torque to drive the synthesized mechanism.

1 Introduction

After the invention of aircraft, human being has desired more and gone through several structural changes in order to increase the aerodynamic efficiency of aircrafts. Since the principal control elements of the aircraft are generally located on the wings, those structural changes have been considered for aircraft wings [1]. Due to the fact that the conventional control surfaces cause a sudden change in the pressure distribution at the hinge line. This usually associated with several drawbacks and the so called “wing morphing” offers more

* Corresponding author: hlsahin@metu.edu.tr

effective and efficient means by providing an adaptive wing structure. This in turn offer radical shape changes in order to produce optimum performance over an aircraft's nominal operational envelope [2], even expand its operating envelope [3].

Generally, there are three accepted major groups for morphing aircraft concepts which are: "planform alternation", "airfoil adjustment" and "out-of-plane transformation" [4]. Among those, the airfoil adjustment is the most widely studied. Airplanes generally adjust the airfoil camber by deflecting the conventional control surfaces. Since the trailing edge bears less aerodynamic moment than the leading edge, it is a lot easier to drive and control [5].

In this paper, the dynamic force analysis of a novel morphing wing trailing edge structure with various configurations of airfoil shapes are conducted. First of all, a SSM is synthesized which satisfies baseline and target airfoil shapes [6]. Then, the aerodynamic analyses of airfoil configurations are performed in 2D by XFOIL, which predicts the pressure distribution over the airfoil which can be integrated to calculate the required torque [7]. In this study, the leading edges of the considered wings have also been assumed to morph in order to achieve the necessary airfoil shapes. In this study, after completing the kinematic analysis of the SSM, the dynamic force analysis of the mechanism under aerodynamic loading have been performed in order to calculate the required torque to drive the mechanism.

2 Theory

The deployable structures (a.k.a. structural mechanisms), are currently used in aerospace applications due to providing large geometrical shape changes [8].

In this paper, a planar "scissor-structural mechanism" (SSM), which is the most popular type of deployable structures, is designed in order to morph the camber line and chord length of an aircraft wing. The planar scissor-structural mechanisms are formed by a series of scissor-like elements (SLEs).

In its basic form of a scissor-like element (SLE), two straight bars or links are connected to each other with a revolute joint [9], and take different forms if imaginary lines ("t-lines"), which get through the hinge locations, differ. For example, if those "t-lines" are parallel throughout the deployment, then such type of elements is called "translational-SLEs"; otherwise, called "polar-SLEs", according to resulting type of motion (translational or curvilinear). A SSM for trailing edge of aircraft wings was previously synthesized by using only translational units [10]. SLEs acquire their prevalence by their inverse-proportional feature between their thickness and width. This relation can be described a "foldability vector" which connects midpoints of two consecutive SLEs [11]. It can be seen that, by changing the type of SLE, such inverse relation can take a complex form, which are used to stretch/ shrink/ bend any geometry in any direction.

2.1 Kinematic analysis of scissor-structural mechanisms

In Fig. 1, a general planar SSM, consisting of translational and polar SLEs, is shown. If a four-bar linkage is assumed to be attached to manipulate the whole SSM from a hinge (i.e C_1), the system becomes a 1-DOF (degree-of-freedom) mechanism. In order to investigate the designed scissor-like mechanism in terms of its dynamic characteristics, the kinematic analysis of the mechanism should be done properly. Assuming that the output angle of the four-bar linkage in terms of time is known; then, the position, velocity and acceleration analyses of whole SSM can be done in terms of that output angle (i.e. γ_0).

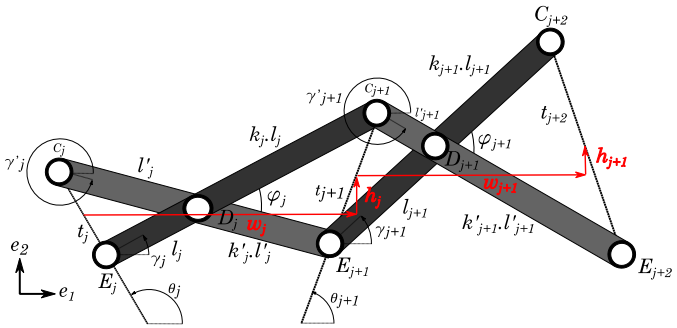

Fig. 1. A general planar SSM consisting of translational and polar SLEs [6].

Considering Fig. 1. and the methodology outlined in [6], the following equation can be obtained:

$$k_j l_j e^{i\varphi_j} + l'_{j+1} e^{i\mu'_{j+1}} = k'_j l'_j + l_{j+1} e^{i\mu_{j+1}} \tag{1}$$

When the angular velocity and acceleration of link $l_j(1+k_j)$ of initial SLE are prescribed, (i.e. $\dot{\gamma}_1, \ddot{\gamma}_1$), then the link $l'_j(1+k'_j)$ behaves as a fixed link ($\dot{\gamma'}_1 = \ddot{\gamma'}_1 = 0$). Then, taking the *first derivative* of the equation (1) with respect to time gives:

$$k_j l_j \dot{\varphi}_j e^{i\varphi_j} + l'_{j+1} \dot{\mu}'_{j+1} e^{i\mu'_{j+1}} = l_{j+1} \dot{\mu}_{j+1} e^{i\mu_{j+1}} \tag{2}$$

Then, manipulating and writing the equation (2) in matrix form, which gives angular velocities of SLEs:

$$[A]\{\dot{\mu}\} = \dot{\varphi}_j \{B_v\} \tag{3}$$

where $[A]$ is known as "characteristic matrix", $\{\dot{\mu}\}$ is the unknown angular velocity vector and $\{B_v\}$ is the known vector:

$$[A] \equiv \begin{bmatrix} l_{j+1}\cos\mu_{j+1} & -l'_{j+1}\cos\mu'_{j+1} \\ l_{j+1}\sin\mu_{j+1} & -l'_{j+1}\sin\mu'_{j+1} \end{bmatrix} \tag{4}$$

$$\{\dot{\mu}\} \equiv \begin{Bmatrix} \dot{\mu}_{j+1} \\ \dot{\mu}'_{j+1} \end{Bmatrix} \tag{5}$$

$$\{B_v\} \equiv \begin{Bmatrix} k_j l_j \cos\varphi_j \\ k_j l_j \sin\varphi_j \end{Bmatrix} \tag{6}$$

Taking the *second derivative* of the equation (1) with respect to time gives:

$$\begin{aligned} k_j l_j \ddot{\varphi}_j e^{i\varphi_j} + i k_j l_j (\dot{\varphi}_j)^2 e^{i\varphi_j} + l'_{j+1} \ddot{\mu}'_{j+1} e^{i\mu'_{j+1}} + i l'_{j+1} (\dot{\mu}'_{j+1})^2 e^{i\mu'_{j+1}} \\ = l_{j+1} \ddot{\mu}_{j+1} e^{i\mu_{j+1}} + i l_{j+1} (\dot{\mu}_{j+1})^2 e^{i\mu_{j+1}} \end{aligned} \tag{7}$$

Then, manipulating and writing the equation (7) in matrix form, which gives angular accelerations of SLEs:

$$[A]\{\ddot{\mu}\} = \{B_a\} \tag{8}$$

where $\{\dot{\mu}\}$ is unknown angular velocity vector and $\{B_a\}$ is the known vector, which are:

$$\{\ddot{\mu}\} \equiv \begin{Bmatrix} \ddot{\mu}_{j+1} \\ \ddot{\mu}'_{j+1} \end{Bmatrix} \tag{9}$$

$$\{B_a\} \equiv \begin{Bmatrix} k_j l_j \ddot{\varphi}_j \cos\varphi_j - k_j l_j \dot{\varphi}_j^2 \sin\varphi_j + l_{j+1}\dot{\mu}_{j+1}^2 \sin\mu_{j+1} - l'_{j+1}\dot{\mu}'^2_{j+1} \sin\mu'_{j+1} \\ k_j l_j \ddot{\varphi}_j \sin\varphi_j + k_j l_j \dot{\varphi}_j^2 \cos\varphi_j - l_{j+1}\dot{\mu}_{j+1}^2 \cos\mu_{j+1} + l'_{j+1}\dot{\mu}'^2_{j+1} \cos\mu'_{j+1} \end{Bmatrix} \quad (10)$$

2.2 Dynamic force analysis of scissor-structural mechanisms

When the inertia forces are also considered in the analysis of the mechanism, the analysis is known as the "dynamic force analysis".

For SSMs, the derivation of equations for only one scissor-like element is sufficient in order to calculate the characteristics of the whole system. Fig. 2 shows the arbitrary locations of the mass centers of a generic scissor-like element.

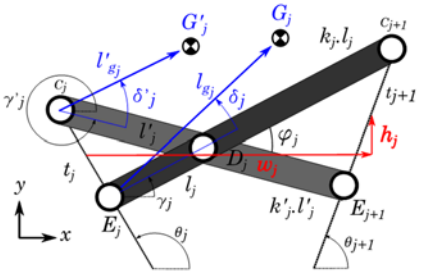

Fig. 2: Representation of arbitrary locations of mass centers of a generic SLE.

In Fig. 2, G_j' and G_j represent the mass centers of links that construct a SLE, l_{g_j}', l_{g_j} and δ_j', δ_j represent the position vectors of the mass centers, and the angle between the corresponding link and the mass center vector of that corresponding link respectively.

Σφάλμα! Το αρχείο προέλευσης της αναφοράς δεν βρέθηκε.a shows the internal and external forces and moment on a generic SLE while Fig. 3b shows inertia forces and moment of the same element.

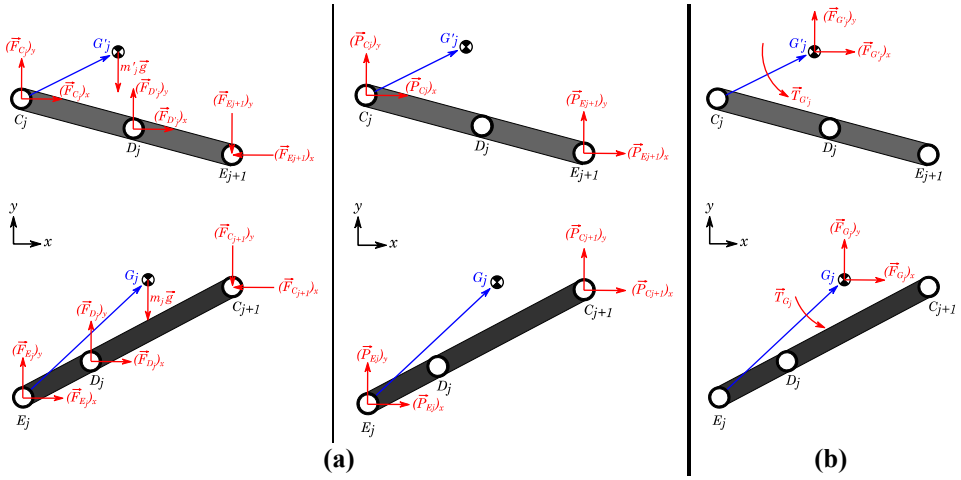

Fig. 3: Free-body-diagram of a SLE: **(a)** internal-external forces, **(b)** effective forces.

Since the SSM has free ends (i.e. $\vec{F}_{C_{N+1}} = \vec{F}_{E_{N+1}} = \vec{0}$), internal forces on the revolute joints can be calculated solving the equation (11) starting from the N^{th} SLE to the 1^{st} SLE (in the opposite direction of the kinematic analysis). The mathematical system represented by equation (11) should be constructed for every SLE separately.

$$\{f\} = [A_f]^{-1}\{B_f\} \tag{11}$$

The dynamic force analysis have been achieved by solving equation (11) at different time steps. The force vector, $\{f\}$, is:

$$\{f\} = \left\{ \left(F_{C_j}\right)_x \quad \left(F_{D_j}\right)_x \quad \left(F_{E_j}\right)_x \quad \left(F_{C_j}\right)_y \quad \left(F_{D_j}\right)_y \quad \left(F_{E_j}\right)_y \right\}^T \tag{12}$$

Using trigonometric identities, the matrix $[A_f]$ can be constituted as:

$$[A_f] = \begin{bmatrix} 1 & -1 & 0 & 0 & 0 & 0 \\ 0 & 1 & 1 & 0 & 0 & 0 \\ 0 & 0 & 0 & 1 & -1 & 0 \\ 0 & 0 & 0 & 0 & 1 & 1 \\ l'_{a_j}\, s(\gamma'_j + \delta'_j) & -g_{a'_j}\, s\left(\eta_{a'_j}\right) & 0 & -l'_{a_j}\, c(\gamma'_j + \delta'_j) & g_{a'_j}\, c\left(\eta_{a'_j}\right) & 0 \\ 0 & g_{b_j}\, s\left(\eta_{b_j}\right) & l_{a_j}\, s(\gamma_j + \delta_j) & 0 & -g_{b_j}\, c\left(\eta_{b_j}\right) & -l_{a_j}\, c(\gamma_j + \delta_j) \end{bmatrix} \tag{13}$$

where $\mathrm{s}(x) \equiv \sin(x)$ and $\mathrm{c}(x) \equiv \cos(x)$. The known vector $\{B_f\}$ can be constituted as:

$$\{B_f\} = \begin{Bmatrix} \left(F_{C'_j}\right)_x + \left(F_{E_{j+1}}\right)_x - \left(P_{C_j}\right)_x - \left(P_{E_{j+1}}\right)_x \\ \left(F_{C_j}\right)_x + \left(F_{C_{j+1}}\right)_x - \left(P_{E_j}\right)_x - \left(P_{C_{j+1}}\right)_x \\ \left(F_{C'_j}\right)_y + \left(F_{E_{j+1}}\right)_y - \left(P_{C_j}\right)_y - \left(P_{E_{j+1}}\right)_y + m'_j g \\ \left(F_{C_j}\right)_y + \left(F_{C_{j+1}}\right)_y - \left(P_{E_j}\right)_y - \left(P_{C_{j+1}}\right)_y + m_j g \\ T_{C'_j} - l'_{a_j}\left(P_{C_j}\right)_x s(\gamma'_j + \delta'_j) + l'_{a_j}\left(P_{C_j}\right)_y c(\gamma'_j + \delta'_j) + g_{E_{j+1}}\left(\left(F_{E_{j+1}}\right)_x - \left(P_{E_{j+1}}\right)_x\right) s\left(\eta_{E_{j+1}}\right) - g_{E_{j+1}}\left(\left(F_{E_{j+1}}\right)_y - \left(P_{E_{j+1}}\right)_y\right) c\left(\eta_{E_{j+1}}\right) \\ T_{C_j} - l_{a_j}\left(P_{E_j}\right)_x s(\gamma_j + \delta_j) + l_{a_j}\left(P_{E_j}\right)_y c(\gamma_j + \delta_j) + g_{C_{j+1}}\left(\left(F_{C_{j+1}}\right)_x - \left(P_{C_{j+1}}\right)_x\right) s\left(\eta_{C_{j+1}}\right) - g_{C_{j+1}}\left(\left(F_{C_{j+1}}\right)_y - \left(P_{C_{j+1}}\right)_y\right) c\left(\eta_{C_{j+1}}\right) \end{Bmatrix} \tag{14}$$

After all the internal forces and moments have been calculated, the required driving torque value of the attached four bar mechanism can be determined. In equation (14) F denotes the internal forces and P stands for the pressure, aerodynamic loading; hence the same equation can also be used for the calculation of in-vacuo conditions by simply assigning $P's$ equal to zero.

3 Results

3.1 Design, aerodynamic modelling and analysis of SSMs for chord and camber morphing wing

The wing and the control surfaces studied here are those of [6]. As an example only those with SLE number $N = 10$ are studied. NACA 2412, NACA 6412 and NACA 8412 cases are analyzed which had the mean design errors of 0.15%, 0.08% and 0.17% respectively [6].

In Fig. 4, a SSM with $N = 10$ SLEs at its initial and final positions are shown. When the anchor link is rotated from $\gamma_0 = 89.7°$ to $\gamma_0 = 72.5°$ (clockwise), the designed SSM satisfied the NACA 8412 geometry with 0.17% mean structural error.

In order to verify the aerodynamic performance, the aerodynamic analyses have also been conducted and they are those of [7]. Again only those with SLE number $N = 10$ are studied. Hence, NACA 2412, NACA 6412 and NACA 8412 cases are analyzed which had the RMS errors of pressure distributions of 0.0575, 0.3047 and 0.1434 respectively [7].

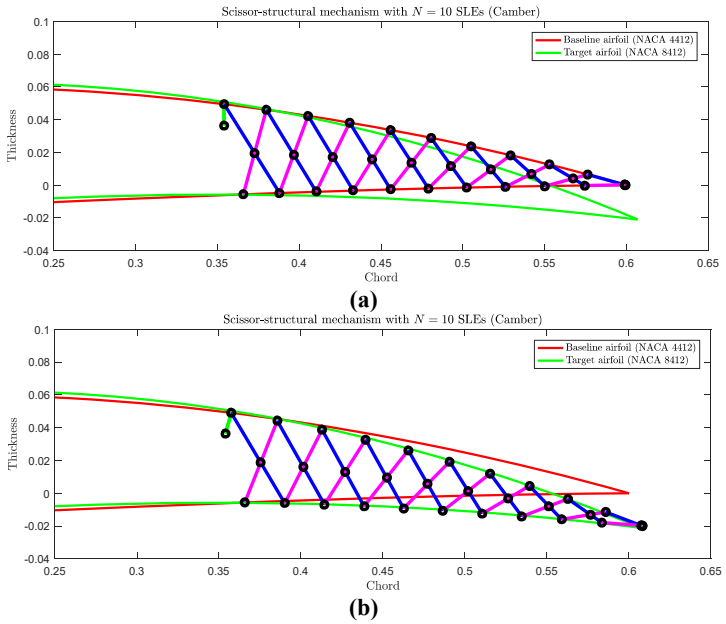

Fig. 4. Scissor-structural mechanism with $\boldsymbol{N = 10}$ SLEs at its **(a)** initial and **(b)** final position**.**

3.2 Kinematic analysis of SSMs for chord and camber morphing wing

In Fig. 5, angular velocities and accelerations of selected links of the proposed SSM with $N = 10$ SLEs are shown for the maximum constant initial velocity of anchor link $\dot{\gamma}_0 = 40$ [rpm].

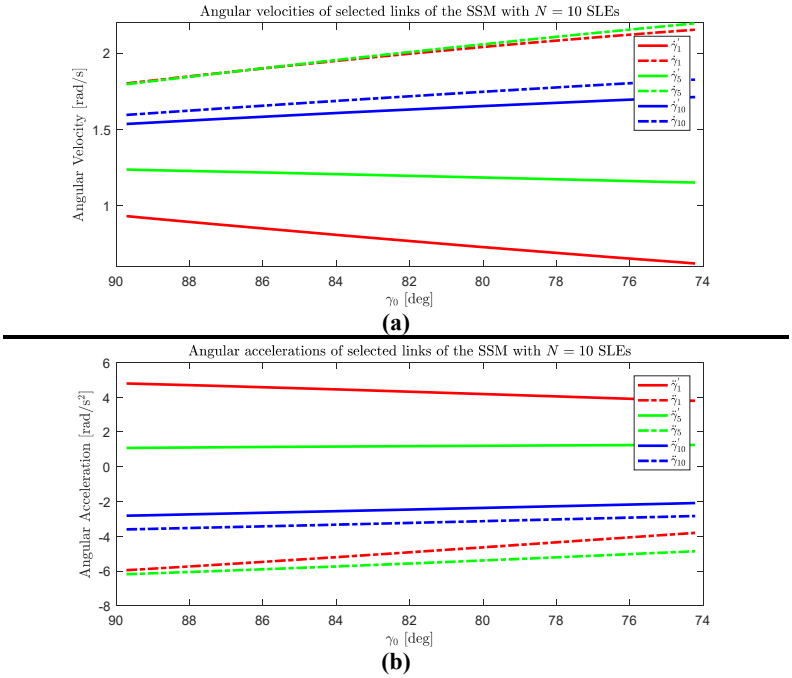

Fig. 5: Angular **(a)** velocities and **(b)** accelerations of selected links of the SSM with $\boldsymbol{N = 10}$ SLEs.

As it can be seen from Fig. 5, the angular velocities and accelerations represent a more or less constant behavior which is desired.

3.3 Dynamic force analysis of SSMs for chord and camber morphing wing

In Fig. 6, magnitudes of internal forces of selected links and the required torque to drive the whole SSM with N=10 SLEs are shown respectively. The masses of the links are calculated for aluminum, $\rho_{Al} = 2700\ \left[\frac{\text{kg}}{\text{m}^3}\right]$. The volumes of links and their moment of inertias are calculated assuming that the links are those of rectangular beams with square cross-section. Both sides of each unique element are 1/5 of its length; therefore, the cross-section of each element is different. By considering these parameters, the weight penalty of the mechanism brought to the wing is 183 [gr].

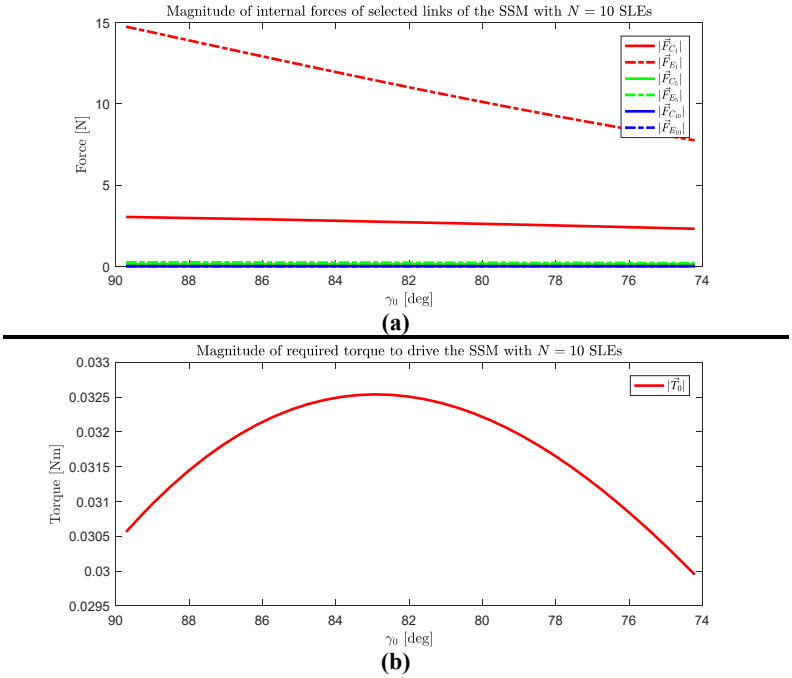

Fig. 6: Magnitudes of **(a)** internal forces of selected links and **(b)** the required torque to drive the whole SSM with $\boldsymbol{N = 10}$ SLEs.

It can be seen from Fig. 6a that only the links close to the torque application have some internal forces due to the applied torque, whereas the other links carry almost zero internal forces. The main characteristics of these type of structural-mechanisms is their being of stress-strain free state. The computed very low internal forces and moments verify this.

Fig. 6b gives a torque value which is below 0.33 [Nm]. This value found to be lower than the torque value of 0.4 [Nm] [12], and further verifies the results of the study.

4 Conclusion

In this article, the design, analysis and synthesis of a deployable mechanism for morphing of the trailing edge of an aircraft wing is presented. Assuming that the wing skin is fully compliant, a scissor-structural mechanism for the morphing of trailing edge of an aircraft wing is synthesized.

The obtained results are compared with the original NACA airfoils, and it is seen that designed scissor-structural mechanisms for each case satisfy the target airfoil profiles successfully with little lift penalty.

Furthermore, kinematic analysis, including velocity and acceleration analyses, have been undertaken in order to determine the inertial forces and moments. The dynamic force analysis of the designed SSM have also been performed in order to compute the required torque value necessary for driving the whole SSM. The computations yielded satisfactory results.

References

[1] S. Barbarino, O. Bilgen, R. M. Ajaj, M. I. Friswell, and D. J. Inman, "A Review of Morphing Aircraft," *J. Intell. Mater. Syst. Struct.*, vol. 22, no. 9, pp. 823–877, 2011.

[2] J. H. S. Fincham and M. I. Friswell, "Aerodynamic optimisation of a camber morphing aerofoil," *Aerosp. Sci. Technol.*, vol. 43, pp. 245–255, 2015.

[3] K. R. Olympio and F. Gandhi, "Flexible skins for morphing aircraft using cellular honeycomb cores," *J. Intell. Mater. Syst. Struct.*, vol. 21, no. 17, pp. 1719–1735, 2010.

[4] A. Y. N. Sofla, S. A. Meguid, K. T. Tan, and W. K. Yeo, "Shape morphing of aircraft wing: Status and challenges," *Mater. Des.*, vol. 31, no. 3, pp. 1284–1292, 2010.

[5] P. Zhang, L. Zhou, W. Cheng, and T. Qiu, "Conceptual Design and Experimental Demonstration of a Distributedly Actuated Morphing Wing," *J. Aircr.*, vol. 52, no. 2, pp. 452–461, 2015.

[6] H. L. Şahin and Y. Yaman, "Design and Analysis of a Novel Mechanism for the Morphing of Trailing Edge of an Aircraft Wing," in *5th International Conference of Engineering Against Failure*, 2018.

[7] H. L. Şahin, B. O. Çakır, and Y. Yaman, "Aerodynamic Modelling and Analysis of a Novel Mechanism for Chord and Camber Morphing Wing," *MATEC Web Conf.*, vol. 188, 2018.

[8] F. Maden, K. Korkmaz, and Y. Akgün, "A review of planar scissor structural mechanisms: Geometric principles and design methods," *Archit. Sci. Rev.*, vol. 54, no. 3, pp. 246–257, 2011.

[9] K. Roovers and N. De Temmerman, "Deployable scissor grids consisting of translational units," *Int. J. Solids Struct.*, vol. 121, pp. 45–61, 2017.

[10] H. L. Şahin and Y. Yaman, "Design and Analysis of a Mechanism for the Chord and Camber Morphing of an Aircraft Wing," in *7th EASN International Conference on Innovation in European Aeronautics Research*, 2017.

[11] C. J. Gantes, J. J. Connor, R. D. Logcher, and Y. Rosenfeld, "Structural analysis and design of deployable structures," *Comput. Struct.*, vol. 32, no. 3–4, pp. 661–669, 1989.

[12] G. B. Spirlet, "Design of Morphing Leading and Trailing Edge Surfaces for Camber and Twist Control," Delft University of Technology, 2015.